Increased thermal stability of a poled electro-optic polymer using high-molar-mass fractions

Ralph P. Bertram,* Nils Benter, Dirk Apitz, Elisabeth Soergel, and Karsten Buse
Physikalisches Institut, Universität Bonn, Wegelerstraße 8, 53115 Bonn, Germany

Rainer Hagen and Serguei G. Kostromine
BAYER MaterialScience AG, 51368 Leverkusen, Germany
(Received 21 June 2004; published 28 October 2004)

Polymer fractionation yields materials with higher average molar masses and thus substantially increased glass transition temperatures. We apply this technique to a photoaddressable polymer that exhibits high electro-optic coefficients, in order to enhance the thermal stability of the poled material. The degree of orientation of the dipolar chromophores is investigated with both pyroelectric and electro-optic measurements. The pyroelectric measurements at elevated temperatures show no significant contribution of β relaxation as compared to α relaxation.

DOI: 10.1103/PhysRevE.70.041802 PACS number(s): 42.70.−a, 42.70.Jk, 77.22.Ej, 77.70.+a

I. INTRODUCTION

The use of polymers for nonlinear optical applications such as second-harmonic generation and electro-optic modulation has been studied intensely for more than two decades. Huge progress has been made in synthesizing chromophores with large hyperpolarizabilities and in poling the materials efficiently [1–3]. In recent years, an increased interest in electro-optic polymers could be noticed, because in conventionally used crystalline materials there are fundamental bandwidth limitations, attributed to optical phonons [1,4]. This limitation does not apply to polymers [5], and electro-optic modulation at bandwidths higher than 100 GHz has been demonstrated [6]. The magnitude of the Pockels effect in polymers can even exceed the one in crystals and the favorable dielectric properties of polymers allow longer interaction lengths in high-speed modulators. Thus, the use of polymers can significantly reduce driving voltages for electro-optic devices [2].

Side chain polymers with azobenzene-based chromophores are also known as photoaddressable polymers (PAP's) because they show a light-induced birefringence Δn that is of special interest for optical data storage [7,8]. The large and stable Δn values originate from cooperative reorientation and alignment of side chains triggered by trans-cis-trans isomerization transitions of the azobenzene molecules after absorption of polarized light of a suitable wavelength [9–12]. This effect can be used for the light-induced formation of waveguiding structures and for the enhancement of the poling efficiency at temperatures well below the glass transition, as well as for spatially patterned poling [13–15]. Recently, we have demonstrated a very strong electro-optic effect in a photoaddressable polymer having bis-azo chromophore side chains with the chemical structure shown in Fig. 1 [16].

The major objection to polymeric components is the device reliability, which is in the case of electro-optic polymers mainly affected by the stability of the polar orientation of the chromophores. Cross-linking the oriented chromophores after poling can lock the molecules in place and thus greatly enhance the stability to an extent that makes first commercial products possible [17]. In this article, we demonstrate a different approach to improve device stability that can be used independently or in addition to a cross-linking procedure.

The thermal stability of a poled polymer is mainly determined by its glass transition temperature T_g. In order to have a long-term stable electro-optic device, T_g needs to be significantly higher than the intended operating temperature. For commercial devices long-term stability at 85 °C is required [3]. The glass transition temperature can be controlled by fractionation—i.e., the separation of macromolecules with different molar masses. For a narrow distribution of molar masses T_g can be expressed as [18]

$$T_g(M_w) = T_g(M_w = \infty) - \frac{K}{M_w}, \tag{1}$$

where K is a constant depending on material parameters and M_w is the weight average of the molar mass distribution function. This behavior can be understood as follows: For lower molar masses the influence of the end groups reduces the glass transition temperature. Increasing the chain length, the end groups become less significant, resulting in an increase of T_g and finally in a saturation, approaching $T_g(M_w=\infty)$. Thus, the use of high-M_w fractions yields significantly higher glass transition temperatures, compared to low-M_w fractions and to the non fractionated polymer.

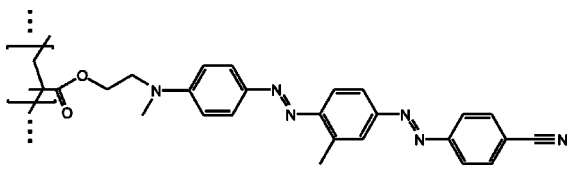

FIG. 1. Chemical structure of the investigated material.

*Electronic address: bertram@physik.uni-bonn.de
URL: www.physik.uni-bonn.de/hertz

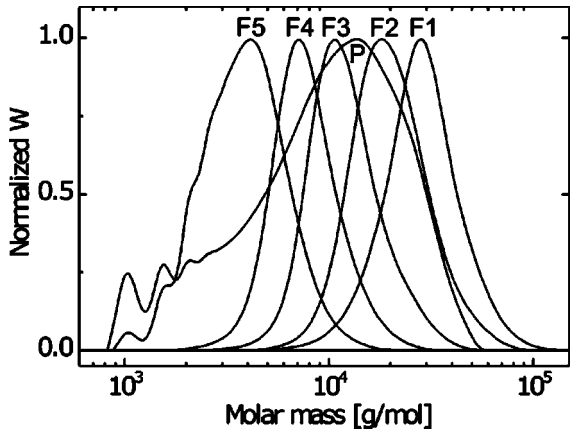

FIG. 2. Molar mass distribution function W (normalized) of the original polymer (P) and its fractions F1–F5. The curves have been obtained in an analytical gel-permeation-chromatography experiment in N,N-dimethylacetamide at 40 °C under consideration of the standard PMMA calibration.

II. EXPERIMENTS

In earlier measurements it has been demonstrated that a strong electro-optic effect can be found in PAP's even with very high chromophore contents [16]. We decided to use the homopolymer with the chemical structure shown in Fig. 1 for further investigations. The polymer is formed by radical polymerization of the monomers in 10 wt % DMF solution during 48 h at 70 °C in an argon atmosphere using azo-bis-isobutironitrile (AIBN) as an initiator. After the polymerization has finished, the solvent is completely evaporated, the polymer boiled in methanol 3 times for 1 h and then dried under vacuum (10^{-3} mbar) for 3 h at 120 °C. The glass transition temperature of this material is determined to be 94 °C by standard differential scanning calorimetry (DSC) measurements with a heating rate of 20 K/min. The fractionation is done in five subsequent steps from a 1 wt % solution of the polymer in THF by addition of a suitable amount of ethanol. Each time the precipitated fraction F1–F5 is collected and dried. Details of the fractionation technique have been published in Ref. [19].

The five fractions have molar mass distributions as shown in Fig. 2. The glass transition temperatures of the fractions range from 99 to 121 °C as listed in Table I. The small and very constant heterogeneity index M_w/M_n, the ratio of weight average to number average molar mass, indicates a successful fractionation with well-defined properties of the resulting materials [18].

The polymer fractions are now solved in cyclopentanone and spin coated to film thicknesses of 0.5–1.0 μm onto glass slides covered by an indium-tin-oxide (ITO) electrode. We use corona poling to break the inversion symmetry of the polymer. Here, special care is taken to maintain a low cooling rate of 1 °C/min when cooling down from the poling temperature in order to minimize local free volumes in the material. After poling, a 150-nm-thick gold layer serving as the second electrode is sputtered on top of the polymer film. These samples are investigated in a free-beam Mach-Zehnder interferometer to measure the electro-optic effect. For simplicity and increased accuracy these measurements are performed at a wavelength of 685 nm. The previously measured dispersion relation for the electro-optic effect in our chromophores allows a rather accurate determination of the Pockels coefficient r_{33} at the technologically important wavelength of 1550 nm. A detailed description of the sample preparation and the interferometric measurement method is given in Ref. [16]. For each fraction more than ten samples are poled and measured to find the optimum poling temperature. Two well-poled samples of the original polymer and of the fraction F2 are stored in an oven at 90 °C, and the remaining electro-optic effect is determined in regular intervals.

For detailed investigation of the chromophore relaxation near the glass transition temperature we measure the pyroelectric effect: The thermal expansion of the material containing oriented molecular dipoles generates an accumulated charge Q on the electrode area A that can be measured as a pyroelectric current [20]. The experimental pyroelectric coefficient $p_{\mathrm{expt}}=(1/A)(\partial Q/\partial T)$ can be related to the macroscopic dipole orientation parameter $\langle\cos\theta\rangle$ (θ being the angle between the direction of the poling field and the individual molecular dipole moment having a magnitude d) via the polarization P as [21]

$$p_{\mathrm{expt}} = \alpha\frac{\epsilon+2}{3}P = \alpha\frac{(\epsilon+2)^2}{9}\frac{N}{V}d\langle\cos\theta\rangle. \qquad (2)$$

Here ϵ is the dielectric constant at low frequencies, α is the thermal expansion coefficient, and N/V is the number density of dipoles in the film. For moderate orientation of dipolar chromophores, the oriented gas model [22] predicts the polarization P and thus p_{expt} to be directly proportional to the

TABLE I. Average molar mass M_w, heterogeneity index M_w/M_n, glass transition temperature T_g, optimum poling temperature T_{pol}, Pockels coefficient r_{33} at 1550 nm, and the curve-fit stretching exponent β for the original material and for the fractions F1–F5.

Material	M_w (g/mol)	M_w/M_n	T_g (°C)	T_{pol} (°C)	r_{33} (pm/V)	β
Original Polymer	13600	2.26	94	102	42	0.23
Fraction 1	33500	1.30	121	128	21	0.22
Fraction 2	23700	1.24	120	124	34	0.23
Fraction 3	14100	1.21	116	120	29	0.16
Fraction 4	8940	1.18	111	117.5	25	0.17
Fraction 5	4580	1.27	99	109	24	0.27

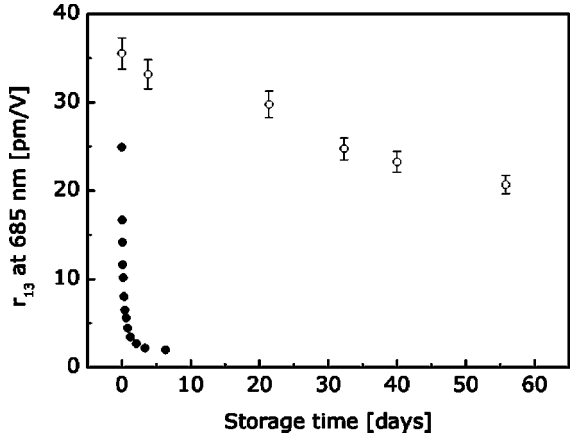

FIG. 3. Pockels coefficients r_{13} measured at 685 nm wavelength for a sample of the nonfractionated material (solid symbols) and a sample of the fraction F2 (open symbols). Both samples are stored in an oven at a temperature of 90 °C and taken out in regular intervals for the interferometric measurements.

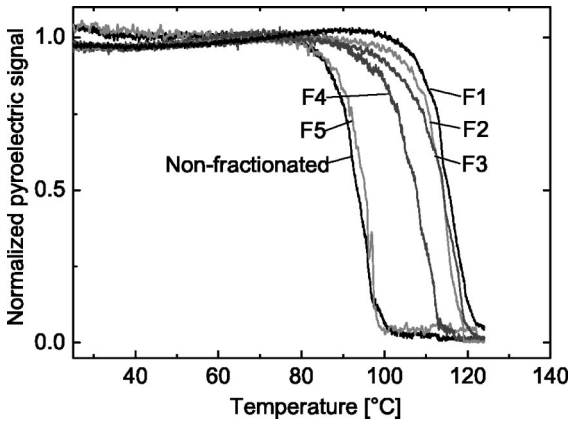

FIG. 4. Pyroelectric signal for a heating rate of (0.2 ± 0.02) °C/min as a function of temperature. The curves are normalized to the signal strength at a temperature of 70 °C and correspond (from right to left) to the fractions F1–F5 and to the nonfractionated polymer.

Pockels coefficients r_{13} and r_{33}. This has also been verified experimentally [23].

When the gold electrode is illuminated with a frequency-doubled $Nd:YVO_4$ laser, about 75% of the laser intensity is absorbed and results in heating the gold electrode, the polymer film, and part of the glass substrate. Placing a chopper wheel into the beam path, the sample is heated periodically, enabling very sensitive lock-in detection. To get accurate information about the pyroelectric current, the signal is measured as a voltage drop over a 10-kΩ load resistor. The sample is mounted on a block of copper that is slowly heated up with a rate of $c=(0.2\pm0.02)$ °C/min. Thus, the temperature dependence of the chromophore order parameter $\langle\cos\theta\rangle$ can be observed directly via the pyroelectric effect. We measure the pyroelectric coefficient continuously over several hours while heating up the sample to 130 °C. Typical laser powers are 10 mW at 3.5 mm beam diameter, and the chopping frequency is 500 Hz in all measurements.

III. EXPERIMENTAL RESULTS

Samples of the five fractions and the nonfractionated polymer are prepared and poled as described above. Optimum poling temperatures and maximum electro-optic coefficients are given in Table I. It is interesting to note that we do not find as large Pockels coefficients in the fractions as in the nonfractionated material; only about 2/3 of the values are observed in the polymer fractions.

The sample of the original polymer, stored at 90 °C, shows a rapid decrease of the Pockels coefficient, as shown in Fig. 3. The Pockels coefficient for the fraction F2 exhibits a much slower decrease. After two months of storage at 90 °C it still retains 2/3 of the original value.

The pyroelectric response versus the average sample temperature is shown in Fig. 4. At temperatures up to 20 °C below the glass transition the pyroelectric effect remains constant, in some samples a slight increase can be seen starting about 50 °C below T_g. The decrease of the pyroelectric coefficient begins about 10 °C below T_g, having a steep slope around the glass transition temperature. Once the sample is heated some degrees above T_g, the pyroelectric effect is permanently removed, indicating complete depolarization of the sample.

IV. DISCUSSION

A. Enhanced lifetime of the poling

The delayed relaxation of the Pockels coefficient through the use of the high-molar-mass fraction F2 is clearly seen in the interferometric measurements shown in Fig. 3. This demonstrates the improvement of thermal stability by increasing M_w through fractionation.

An independent method for evaluation of the thermal stability of poled polymers is pyroelectric measurements at elevated temperatures. The measurement results show a slight increase of the pyroelectric coefficient upon approaching T_g in some curves of Fig. 4. This effect has also been observed by other authors [23] and may be related to an additional contribution of torsional vibration ("libration") of the dipoles to the pyroelectric effect when the dipoles see greater local free volumes at elevated temperatures [21]. At even higher temperatures the pyroelectric effect decreases rapidly. Here, the correlation between the increased thermal stability of the polymer fractions and the enhanced glass transition temperature is clearly visible: The decay of the pyroelectric effect in fractions with increased molar mass happens at higher temperatures. It is interesting to note that also the polymer fractions with the lowest average molar masses (F4 and F5) show a better thermal stability than the nonfractionated material (see Fig. 4). The reason is probably, that the nonfractionated material contains very short polymer chains (1–4 monomer units, molar mass below 2000 g/mol; see Fig. 2) that reduce the glass transition temperature by acting as plasticizers.

The origin of the reduced Pockels coefficients in the fractions as compared to the original polymer is not yet clear.

One may speculate that in the nonfractionated material the chromophores on very short main chains can be aligned more effectively than those attached to longer polymer backbones.

B. Modeling of the thermal relaxation of the poling

To get a deeper understanding of the relaxation processes involved, however, we must investigate the *shape* of the relaxation curves in Fig. 4. It has been widely accepted that the semiempirical Kohlrausch-Williams-Watts (KWW) function [24,25]

$$n(t) = n(0)\exp[-(t/\tau_{\mathrm{KWW}})^{\beta}] \tag{3}$$

is in a first approximation suitable for fitting a broad variety of relaxational phenomena in disordered materials. This equation describes a parameter n relaxing with time t, with the stretching exponent β ranging from 0 to 1, and the characteristic relaxation time τ_{KWW}. It can be formally explained by assuming a superposition of exponentials,

$$n(t) = n(0)\int_0^{\infty} g(\tau)\exp[-(t/\tau)]\mathrm{d}\tau, \tag{4}$$

where $g(\tau)$ is a distribution of Debye-type relaxation times τ— i.e., simple exponential decays as they appear for $\beta=1$ in Eq. (3).

In experimental observations, the exponent β increases monotonically with temperature and is supposed to reach 1 for very high temperatures [26]. The broader the distribution $g(\tau)$ of the relaxation times (meaning more diverse molecular environments), the lower is this stretching exponent. We would expect that a narrower distribution of molar masses by fractionating leads to a higher homogeneity of local energetic environments. Therefore the more similar microscopic relaxation times yield also a higher value of β.

However, of course not all processes with relaxation time distributions are describable with a stretched exponential function. This happens, e.g., when the distribution function $g(\tau)$ has more than one peak.

In glass-type polymeric materials two different types of relaxation occur: a slow, strongly temperature-dependent relaxation, which is generally associated with main chain rearrangements and referred to as "α relaxation," and a faster, less temperature dependent-relaxation, associated with side group movements and referred to as "β relaxation" [27]. As we slowly increase the temperature in our pyroelectric measurements, the side groups have already relaxed as far as the main chains allow, and without temporal resolution we observe a combined α and β relaxation. As the entire process is described with only one function (KWW), agreement can only be achieved when the distribution peaks of the two different processes are broad and merging enough to be consistent with only one distribution function, which is not the general case for all temperature ranges [28].

Besides the position of the transition in DSC measurements, the glass transition temperature can also be defined as the temperature where the structural relaxation time is of the order of 100 s [29]. Below that temperature the relaxation time diverges. As a first approximation we describe this behavior linearly on a logarithmic scale as follows:

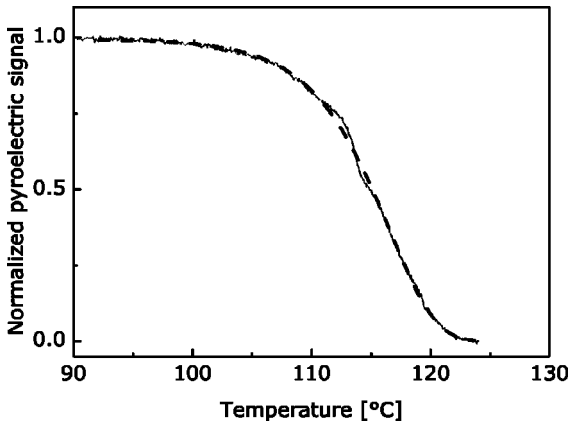

FIG. 5. Normalized pyroelectric signal at a heating rate of (0.2 ± 0.02) °C/min as a function of temperature. The solid line represents measurement data of a sample of the high-T_g fraction F1. The dashed line represents the curve fit.

$$\tau_{\alpha}(T) = 100\ \mathrm{s} \times 10^{a(T_g - T)}, \tag{5}$$

where T is the temperature and a a shape parameter. We argue that, on the one hand, the diverging relaxation times are too high to affect the decay of the orientation during the relatively short time the sample is heated through the region of lower temperatures. On the other hand, when reaching the relaxation time region at high temperatures, the decay has already completed. Between these two regions we are able to apply Eq. (5). Since the major part of the decay happens within 15 °C, as a first approximation the stretching exponent β varies only slightly, and we assume it to be constant during the relaxation process [30]. Since we have a constant heating rate c, we obtain the following curve-fit function for the pyroelectric current I:

$$I(T) = I(0)\exp\left[-\left(\frac{T}{c \times 100\ \mathrm{s} \times 10^{a(T_g - T)}}\right)^{\beta}\right]. \tag{6}$$

For curve fitting we normalize the pyroelectric data to the value 1. Figure 5 shows the data for the high-T_g fraction F1, smoothed and averaged over two samples (solid line), and the curve fit (dashed line). In a first series of curve fits the shape parameter a is let free and leads to an averaged value of about 0.5 K^{-1}. In order to have more precise information on the behavior of the stretching parameter β, in a second run of curve fits, we fix a to the value 0.5 K^{-1} for all curves. With now actually only one free curve-fit parameter (stretching exponent β), using the glass transition temperatures T_g determined by the DSC measurements, we get amazingly good agreement between our intuitive picture and the experimental results even with all the approximations made (Fig. 5).

Comparing the stretching exponents β from all measurements, we find no significant dependence. With two exceptions the values are between 0.23 and 0.27. It is not clear why the two fractions F3 and F4 show significantly lower β values, corresponding to a decay of polarization that is more

flat than the others, while still Eq. (6) fits the experimental data in an excellent manner. Also the unfractionated material ($\beta=0.23$) decays as steeply as the polymers with a less broad distribution of molar mass and substantially lower heterogeneity index M_w/M_n (see Table I). Thus, our first expectation of narrower distributions leading to higher values of β proves wrong. One explanation of this behavior could be that the very slow cooling during the poling process allows the polymer chains to indent strongly with each other by minimizing the free volume. This local indenting seems to strongly affect local environments and to be much more important for relaxation shapes than main chain lengths, which only defines the glass transition temperature. However, the good curve fit suggests that isolated side-chain relaxation is weak, because an additional significant and temporally separated secondary relaxation would make it impossible to simplify Eqs. (3) and (4) while still obtaining good descriptions of the experimental data. Thus, even though we only detect the chromophore side chains in our experiments, their movement must be strongly coupled to neighboring side groups by cooperative orientation and to the main chains, which give way by α relaxation. The prevailing role of α relaxation is the reason why the increased glass transition temperature by using higher M_w fractions increases so significantly the orientation stability.

V. CONCLUSIONS

In conclusion, we have shown that the use of PAP fractions with higher molar masses significantly increases the thermal stability due to higher glass transition temperatures. Having long, densely placed bis-azo chromophore side chains, by poling under suitable conditions the influence of the β relaxation can be very much decreased.

ACKNOWLEDGMENTS

The authors from Universität Bonn thank the Deutsche Forschungsgemeinschaft (Project No. SO 504/1) and the Deutsche Telekom AG for financial support

[1] M. G. Kuzyk and C. W. Dirk, *Characterization Techniques and Tabulations for Organic Non-linear Optical Materials* (Marcel Dekker, New York, 1998).
[2] Y. Shi, C. Zhang, H. Zhang, J. H. Bechtel, L. R. Dalton, B. H. Robinson, and W. H. Steier, Science **288**, 119 (2000).
[3] H. Ma, A. K.-Y. Jen, and L. R. Dalton, Adv. Mater. (Weinheim, Ger.) **14**, 1339 (2002).
[4] L. Eldada, Opt. Eng. **40**, 1165 (2001).
[5] M. Lee, H. E. Katz, C. Erben, D. M. Gill, P. Gopalan, J. D. Heber, and D. J. McGee, Science **298**, 1401 (2002).
[6] D. Chen, H. R. Fetterman, A. Chen, W. H. Steier, L. R. Dalton, W. Wang, and Y. Shi, Appl. Phys. Lett. **70**, 3335 (1997).
[7] T. Todorov, L. Nikolova, and N. Tomova, Appl. Opt. **23**, 4309 (1984).
[8] R. Hagen and T. Bieringer, Adv. Mater. (Weinheim, Ger.) **13**, 1805 (2001).
[9] G. C. Hartley, Nature (London) **140**, 281 (1937).
[10] C. S. Paik and H. Morawetz, Macromolecules **5**, 171 (1972).
[11] M. Eich, J. H. Wendorff, B. Reck, and H. Ringsdorf, Makromol. Chem., Rapid Commun. **8**, 59 (1987).
[12] Y. Q. Shen and H. Rau, Makromol. Chem. **192**, 945 (1991).
[13] M. B. J. Diemeer, F. M. M. Suyten, E. S. Trommel, A. McDonach, J. M. Copeland, L. W. Jenneskens, and W. H. G. Horsthuis, Electron. Lett. **26**, 379 (1990).
[14] Z. Sekkat, J. Wood, E. F. Aust, W. Knoll, W. Volksen, and R. D. Miller, J. Opt. Soc. Am. B **13**, 1713 (1996).
[15] S. Yilmaz, S. Bauer, and R. Gerhard-Multhaupt, Appl. Phys. Lett. **64**, 2770 (1994).
[16] R. P. Bertram, E. Soergel, H. Blank, N. Benter, K. Buse, R. Hagen, and S. G. Kostromine, J. Appl. Phys. **94**, 6208 (2003).
[17] M.-C. Oh, H. Zhang, A. Szep, V. Chuyanov, W. H. Steier, C. Zhang, L. R. Dalton, H. Erlig, B. Tsap, and H. R. Fetterman, Appl. Phys. Lett. **76**, 3525 (2000).
[18] J. M. G. Cowie, *Polymers: Chemistry & Physics of Modern Materials* (Stanley Thornes, Cheltenham, 1991).
[19] S. G. Kostromin, V. P. Shibaev, U. Gessner, H. Cackovic, and J. Springer, Vysokomol. Soedin., Ser. A Ser. B **38**, 1566 (1996).
[20] S. Bauer, J. Appl. Phys. **75**, 5306 (1994).
[21] F. I. Mopsik and M. G. Broadhurst, J. Appl. Phys. **46**, 4204 (1975).
[22] J. W. Wu, J. Opt. Soc. Am. B **8**, 142 (1991).
[23] S. Bauer and S. B. Lang, IEEE Trans. Dielectr. Electr. Insul. **4**, 647 (1996).
[24] R. Kohlrausch, Ann. Phys. (Leipzig) **128**, 1 (1866).
[25] G. Williams and D. C. Watts, Trans. Faraday Soc. **66**, 80 (1970).
[26] J. C. Phillips, Rep. Prog. Phys. **59**, 1133 (1996).
[27] D. Apitz, C. Svanberg, K. G. Jespersen, T. G. Pedersen, and P. M. Johansen, J. Appl. Phys. **94**, 6263 (2003).
[28] R. Bergman, F. Alvarez, A. Alegria, and J. Colmenero, J. Chem. Phys. **109**, 7546 (1998).
[29] M. L. Lee, Y. Li, Y. P. Feng, and W. C. Carter, Phys. Rev. B **67**, 132201 (2003).
[30] K. D. Singer and L. A. King, J. Appl. Phys. **70**, 3251 (1991).